PERGAMON

International Journal of Heat and Mass Transfer 42 (1999) 993–1006

International Journal of HEAT and MASS TRANSFER

Condensation heat transfer and pressure drop of refrigerant R-134a in a plate heat exchanger

Yi-Yie Yan, Hsiang-Chao Lio, Tsing-Fa Lin*

Department of Mechanical Engineering, National Chiao Tung University, Hsinchu, Taiwan

Received 12 March 1998; in final form 19 June 1998

Abstract

An experimental refrigerant loop has been established in the present study to measure the condensation heat transfer coefficient h_r and frictional pressure drop ΔP_f of R-134a in a vertical plate heat exchanger. Two vertical counter flow channels were formed in the exchanger by three plates of commercialized geometry with a corrugated sinusoidal shape of a chevron angle of 60°. Downflow of the condensing R-134a in one channel releases heat to the cold upflow of water in the other channel. The effects of the refrigerant mass flux, average imposed heat flux, system pressure (saturated temperature) and vapor quality of R-134a on the measured data were explored in detail. The results indicate that at a higher vapor quality the condensation heat transfer coefficient and pressure drop are significantly higher. A rise in the refrigerant mass flux only causes a mild increase in the h_r values for most cases. The corresponding rise in the ΔP_f value is slightly larger. Furthermore, it is noted that the condensation heat transfer is only slightly better for a higher average imposed heat flux. But the associated rise in ΔP_f is larger. Finally, at a higher system pressure the h_r value is found to be slightly lower. But the effect of the system pressure on ΔP_f is small. Correlations are also provided for the measured heat transfer coefficients and pressure drops in terms of the Nusselt number and friction factor.

Nomenclature

A heat transfer area of the plate [m^2]
b channel spacing [m]
Bo boiling number, dimensionless, eq. (34)
c_p specific heat [J/kg °C]
D_h hydraulic diameter [m]
f friction factor
g acceleration due to gravity [m/s^2]
G mass flux [kg/m^2 s]
G_{eq} equivalent all liquid mass flux, eq. (35)
h heat transfer coefficient [W/m^2 °C]
i_{fg} enthalpy of vaporization [J/kg]
k conductivity [W/m °C]
L channel length from center of inlet port to center of exit port [m]
LMTD log mean temperature difference [°C]
Nu Nusselt number, dimensionless
P pressure [MPa]
P_c critical pressure [MPa]
Pr Prandtl number
Q heat transfer rate [W]
q_w'' average imposed wall heat flux [W/m^2]
R_{wall} heat transfer resistance of the wall
Re Reynolds number, GD_h/μ_l, dimensionless
Re_{eq} equivalent all liquid Reynolds number, eq. (33)
T temperature [°C]
U overall heat transfer coefficient [W/m^2 °C]
u velocity [m/s]
v specific volume [m^3 kg]
w channel width of the plate [m]
W mass flow rate [kg/s]
X vapor quality.

Greek symbols
ΔP pressure drop
ΔT temperature difference
ΔX total quality change in the exchanger

* Corresponding author. Tel.: +886-35712121-55118; Fax: +886-35720634; E-mail: u8414813@cc.nctu.edu.tw.

PII: S001–7931(09)80021–78

ρ density [kg/m^3]
μ viscosity [N s/m^2].

Subscripts
de deceleration
ave average
c, h at cold side and hot side of the test section
ele elevation
exp experiment
f friction
fg difference between liquid phase and vapor phase
g vapor phase
i, o at inlet and exit of test section
l liquid phase
lat, sens latent and sensible heats
m average value for the two phase mixture or between the inlet and exit
man the test section inlet and exit manifolds and ports
p pre-evaporator
r refrigerant
tp two-phase
w water
wall wall/fluid near the wall.

1. Introduction

It is well recognized that the quick destruction of the ozone layer in the earth atmosphere noted recently has been primarily related to the wide use of the chlorofluorocarbon (CFC) refrigerants, which have been employed as the working fluids in many refrigeration, air conditioning and heat pump systems or as cleansing fluids for processing microelectronic devices. Under the mandate of the Montreal Protocol, the use of CFCs had been phased out and the use of HCFCs will also be phased out in a short period of time. Therefore, we have to replace the CFCs by new alternative refrigerants. In order to properly use these new refrigerants, we need to know their thermodynamic, thermophysical, flow and heat transfer properties. Specifically, we realize that a much more detailed understanding of the flow boiling and condensation heat transfer of new refrigerants (R-134a, R-125, R-152, etc.) is very important in the design of evaporators and condensers used in many current refrigeration and air conditioning systems. In the present study we intend to carry out an experimental study to measure the condensation heat transfer data for the flow of refrigerant R-134a in a vertical plate heat exchanger. In particular, measurements of condensation heat transfer coefficient and pressure drop will be conducted for refrigerant R-134a.

A brief review of literature relevant to the present study is given in the following. For in-tube condensation, Schlager et al. [1] used R-22 as the working fluid and three micro-finned tubes with an outer diameter of 12.7 mm were tested. A smooth tube was also tested to establish a basis for comparison. The average condensation heat transfer coefficients of the micro-finned tubes were 1.5 to 2.0 times larger than those in the smooth tube. Micro-finned tubes having 9.5 mm OD and 8.9 mm maximum ID were also tested [2]. The condensation heat transfer enhancement factors were between 1.4 and 1.8 while the pressure drop penalty factors ranged from 1.0 to slightly higher than 1.2.

Later, Eckels and Pate [3] examined the in-tube flow evaporation and condensation heat transfer for refrigerants R-134a and R-12. The heat transfer coefficients were measured in a horizontal, smooth tube with an inner diameter of 8.0 mm. For similar mass fluxes, R-134a showed a 25 to 35% higher heat transfer coefficient when compared with R-12 for condensation. Torikoshi and Ebisu [4] experimentally investigated evaporation and condensation heat transfer and pressure drop for R-134a, R-32, and a mixture of R-134a/R-32 in a horizontal smooth tube. The condensation heat transfer coefficients for R-32 and R-134a are respectively about 65% and 10% larger than those for R-22 at the same mass flux. For a mixture of R-32 and R-134a, the condensation heat transfer coefficients fall below those for R-22. In the study by Liu [5], condensation and evaporation heat transfer and pressure drop of R-134a and R-22 in a tube were investigated. The condensation heat transfer coefficients for R-134a are 8 to 18% higher and the pressure drop is 50% higher than those for R-22.

Recently, Chamra and Webb [6] tested some advanced micro-finned tubes formed by applying a second set of grooves at the same helix angle but in an opposite angular direction to the first set. They found that the tubes provided 27% higher condensation heat transfer coefficient than the single-helix tube, while the pressure drop was only 6% higher.

Some correlations for estimating in-tube condensation heat transfer coefficient were proposed in the literature. Akers et al. [7] measured average condensation heat transfer coefficients for R-12 and propane inside horizontal tubes. The heat transfer coefficient was found to increase with the vapor velocity. Their experimental data were correlated in terms of an equivalent Reynolds number. Moreover, Shah [8] proposed a correlation for film condensation inside pipes based on a wide variety of experimental data including water, R-11, R-12, R-22 and R-113 in horizontal, vertical and inclined pipes with diameter ranging from 7 to 40 mm.

A close inspection of the literature reviewed above reveals that only some heat transfer characteristics and pressure drop for the in-tube condensation of the new refrigerant R-134a have been investigated. Unfortunately, there are rather limited data available for the design of plate heat exchangers for the condenser application. It is known that the plate heat exchangers (PHE) have been widely used in food processing, chemical reaction processes and other industrial applications for many years. Due to their high efficiency and compactness, the utilization of PHE in refrigeration and air conditioning systems is popular. Some studies about PHE have been reported in the open literature focusing on the single phase liquid to liquid heat transfer [9–11]. But there is little data available for the design of PHE used as evaporators and condensers. In this study, the characteristics of condensation heat transfer and pressure drop for refrigerant R-134a flowing in a plate heat exchanger were explored experimentally.

2. Experimental apparatus and procedures

The experimental system established here to study the condensation of R-134a, as schematically shown in Fig. 1, has four main loops and a data acquisition unit. Specifically, the system includes a refrigerant loop, two water loops (one for pre-evaporator and the other for the test section) and a water–glycol loop. Refrigerant R-134a is circulated in the refrigerant loop. In order to obtain different test conditions of R-134a (including vapor quality, pressure and imposed heat flux) in the test section, we need to control the temperatures and flow rates of the working fluids in the other three loops.

2.1. Refrigerant loop

The refrigerant loop contains a refrigerant pump, an accumulator, a refrigerant mass flow meter, a pre-evaporator, a test section (the plate heat exchanger), a condenser, a sub-cooler, a receiver, a filter/dryer and three sight glasses. The refrigerant pump is a Hydracell pump driven by a DC motor that is, in turn, controlled by a variable DC output motor controller. The variation of the liquid R-134a flow rate was controlled by a rotational DC motor through the change of the DC current. The refrigerant flow rate can also be adjusted by opening the by-pass valve. In the loop, the accumulator connecting to a high-pressure nitrogen tank was used to dampen the fluctuations of the R-134a flow rate and pressure. The refrigerant flow rate was measured by a mass flow meter (Micro motion D25) installed between the pump and pre-evaporator with an accuracy of $\pm 1\%$. The pre-evaporator is used to evaporate the refrigerant to a specified vapor quality at the test section inlet by transferring heat from the hot water to R-134a. Note that the amount of heat transfer from the hot water to the refrigerant in the pre-evaporator is calculated from the energy balance in the water flow. The filter/drier intends to filter the solid particles possibly present in the loop. Meanwhile, a condenser and a sub-cooler were used to condense the

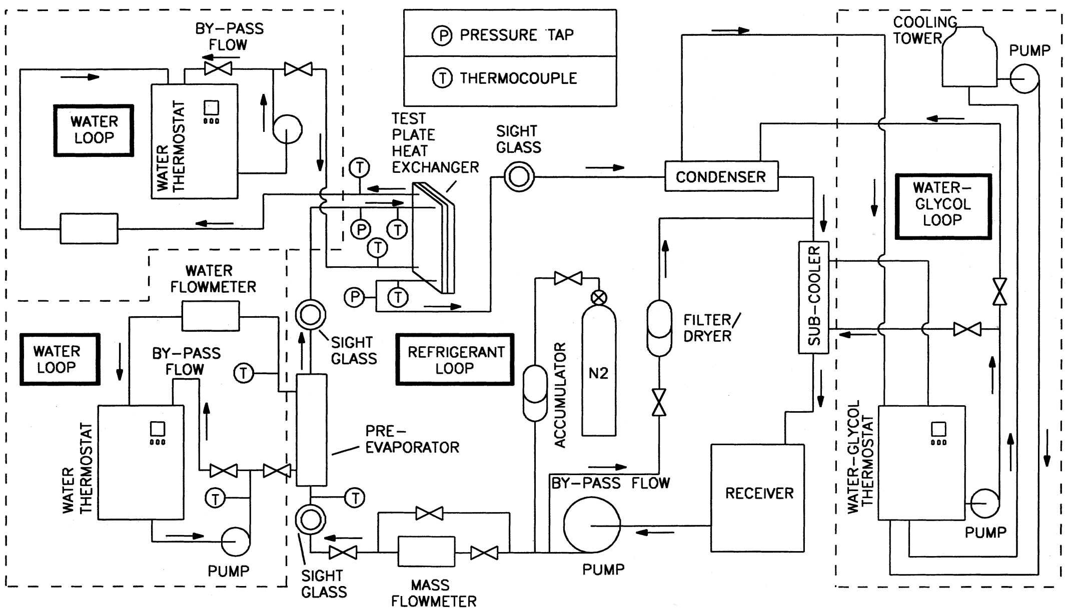

Fig. 1. Schematic diagram of the experimental system.

refrigerant vapor from the test section by a cold water–glycol system to avoid cavitation at the pump inlet. The pressure of the refrigerant loop can be controlled by varying the temperature and flow rate of the water–glycol mixture in the condenser. After condensed, the liquid refrigerant flows back to the receiver.

2.2. Plate heat exchanger: the test section

The plate heat exchanger used in this study, as schematically shown in Fig. 2, was formed by three commercialized SS-316 plates. The plate surfaces were stamped to become grooved with a corrugated sinusoidal shape and 60° of chevron angle. Each plate is 0.4 mm thick and the pitch between the plates is 3.3 mm. The exchanger including the inlet and outlet ports is 500.0 mm long. Note that the distance between the inlet to outlet port centers is 450.0 mm. Each connection port has a diameter of 30.0 mm. The width of the exchanger is 120.0 mm. Moreover, the pitch of the corrugation on each plate from the side view is 10.0 mm. The corrugated grooves on the right and left outer plates have a V shape but the middle plate has a contrary V shape on both sides. This arrangement allows the flow streams to divide into two different flow directions in each channel between the plates and to move along the grooves on the side walls of the channels. Due to the contrary V shapes between two neighbor plates the flow streams near the two plates cross each other in each channel. This cross flow resulting in a significant flow unsteadiness and randomness. In fact, the flow is highly turbulent even at low Reynolds number.

In the heat exchanger the downflow of the refrigerant R-134a in one channel was cooled by the upflow of the cold water in the other channel. To reduce the heat loss to the ambient, the whole test section is wrapped with 10

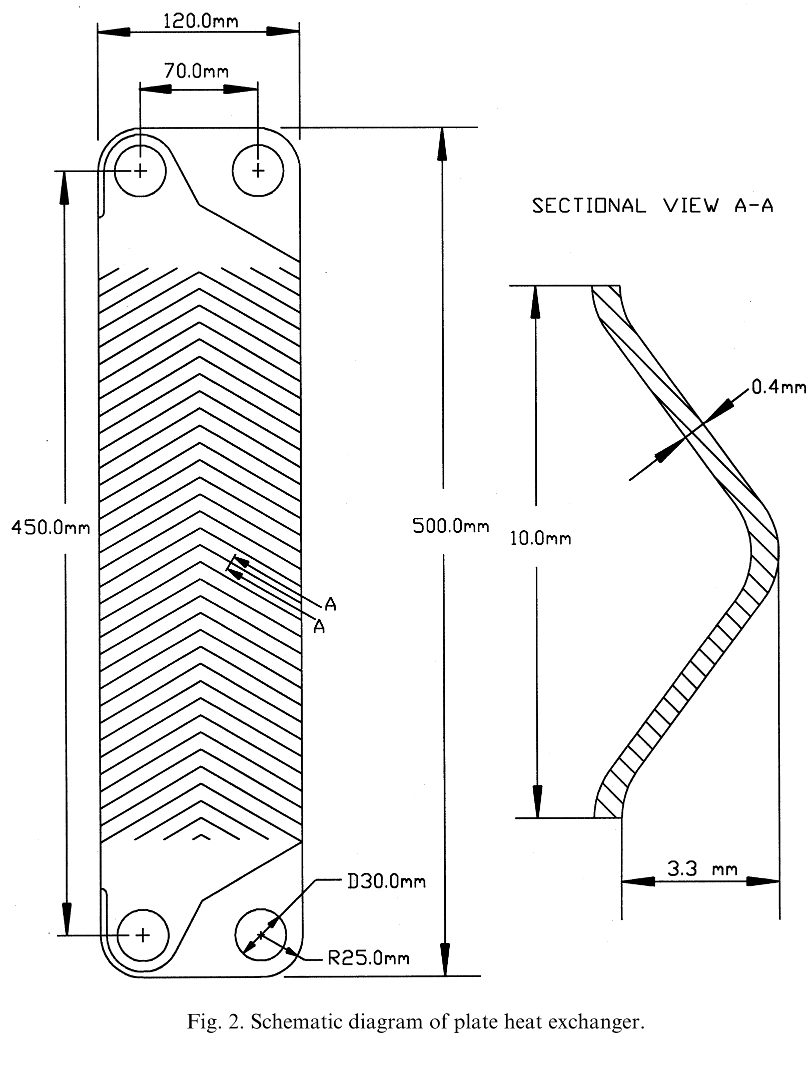

Fig. 2. Schematic diagram of plate heat exchanger.

cm thick polyethylene. The average heat flux in the test section was calculated by measuring the water temperature rise between the channel inlet and outlet and by measuring the water flow rate. The pressure and differential pressure transducers both having accuracy of $\pm 0.5\%$ were also connected to the inlet and outlet of the plate heat exchanger.

2.3. Water loop for test section

The water loop in the system designed for circulating cold water through the test section contains a 200 liter constant temperature water bath with a 4 kW heater and an air cooled refrigeration unit of 3.5 kW cooling capacity intending to accurately control the water temperature. A 0.5 hp water pump with an inverter is used to drive the cold water to the plate heat exchanger with a specified water flow rate. Another by-pass water valve can also be used to adjust the water flow rate. The accuracy of measuring the water flow rate by the flow meter is $\pm 0.5\%$.

2.4. Water loop for pre-evaporator

A double pipe heat exchanger having a heat transfer area of 0.12 m^2 was used as the pre-evaporator. The liquid R-134a flowing in the inner pipe was heated to a specific vapor quality by the hot water flow in the outer annular passage. The pre-evaporator and the connection pipe between the test section and the pre-evaporator were all thermally insulated with 6 cm thick polyethylene. The hot water loop designed for the pre-evaporator consists of a 125 l constant temperature water bath with three 2.0 kW heaters. Then, a 0.5 hp water pump with an inverter is also used to drive the hot water at a specified water flow rate to the pre-evaporator. Similarly, a by-pass water valve is also used to adjust the flow rate. The water flowmeter also has an accuracy of $\pm 0.5\%$.

2.5. Water–glycol loop

The water–glycol loop designed for condensing the R-134a vapor contains another 125 l constant temperature bath with a water cooled refrigeration system. The cooling capacity is 2 kW for the water–glycol at -20°C. The water–glycol at a specified flow rate is driven by a 0.5 hp pump to the condenser as well as to the sub-cooler. A by-pass valve is also provided to adjust the water–glycol flow rate.

2.6. Data acquisition

The data acquisition unit includes a 30 channel YOKOGAWA HR-2300 recorder combined with a personal computer. The recorder was used to record the temperature and voltage data. The water flowmeter and differential pressure transducer need a power supply as a driver to output an electric current of 4–20 mA. The IEEE488 interface was used to connect the controller and the recorder, allowing the measured data to transmit from the recorder to the controller and then to be analyzed by the computer immediately.

2.7. Experimental procedures

In each test the system pressure is maintained at a specified level by adjusting the water–glycol temperature and its flow rate. The vapor quality of R-134a at the test section inlet can be kept at the desired value by adjusting the temperature and flow rate of the hot water loop for the pre-evaporator. Finally, the heat transfer rate between the counter flow channels in the test section can be varied by changing the temperature and flow rate in the water loop for the test section. Any change of the system variables will lead to fluctuations in the temperature and pressure of the flow. It takes about 20–100 min to reach a statistically steady state at which variations of the time-average inlet and outlet temperatures are less than 0.1°C and the variations of the pressure and heat flux are within 1% and 4%, respectively. Then the data acquisition unit is initiated to scan all the data channels for ten times in 40 s. The mean values of the data for each channel are obtained to calculate the heat transfer coefficient and pressure drop. Additionally, the flow rate of water in the test section should be high enough to have turbulent flow in the water side so that the associated single phase heat transfer in it is high enough for balancing the condensation heat transfer in the refrigerant side. In this study, the Reynolds number of the water flow is maintained beyond 200 to insure the flow being turbulent in accordance with the data for the Wilson plot.

Before examining the condensation heat transfer characteristics, a preliminary experiment for single phase water convection in the plate heat transfer exchanger was performed. The Wilson's [12] method was adopted to calculate the relation between single phase heat transfer coefficient and flow rate from these data. This single phase heat transfer coefficient can then be used to analyze the data acquired from the two phase heat transfer experiments.

3. Data reduction

A data reduction analysis is needed in the present measurement to deduce the heat transfer rate from the refrigerant flow to the water flow in the test section. From the definition of the hydraulic diameter, Shah and Wanniarachchi [13] suggested to use two times of the channel spacing as the hydraulic diameter for plate heat exchangers, i.e.

$$D_h \approx 2b \quad \text{for} \quad w \gg b \tag{1}$$

3.1. Single phase water to water heat transfer

In the initial single phase water to water heat transfer test for the plate heat exchanger, the fluid properties were calculated according to the averages of the inlet and outlet bulk fluid temperatures. The energy balance between the hot and cold sides of water were within 2% for all runs, that is

$$Q_{w,h} = W_{w,h} c_{p,w} (T_{w,h,i} - T_{w,h,o}) \tag{2}$$

$$Q_{w,c} = W_{w,c} c_{p,w} (T_{w,c,o} - T_{w,c,i}) \tag{3}$$

and

$$\frac{|Q_{w,h} - Q_{w,c}|}{Q_{ave}} < 2\% \tag{4}$$

with

$$Q_{ave} = \frac{(Q_{w,h} + Q_{w,c})}{2} \tag{5}$$

in which W and c_p are the mass flow rate and specific heat of water, respectively. The overall heat transfer coefficient U between the two counter channel flows of water can be expressed as

$$U = \frac{Q_{ave}}{A\,\text{LMTD}} \tag{6}$$

where the log mean temperature difference (LMTD) is determined from the inlet and exit temperatures of two flow channels:

$$\text{LMTD} = \frac{(\Delta T_1 - \Delta T_2)}{\ln(\Delta T_1/\Delta T_2)} \tag{7}$$

with

$$\Delta T_1 = T_{w,h,i} - T_{w,c,o} \tag{8}$$

$$\Delta T_2 = T_{w,h,o} - T_{w,c,i} \tag{9}$$

In view of the same heat transfer area in the hot and cold sides, the relation between the overall heat transfer coefficient and the convective heat transfer coefficients on both sides can be expressed as

$$\left(\frac{1}{U}\right) = \left(\frac{1}{h_{w,h}}\right) + \left(\frac{1}{h_{w,c}}\right) + R_{wall}A \tag{10}$$

where $h_{w,h}$ and $h_{w,c}$ are respectively the heat transfer coefficients for the hot and cool water sides and R_{wall} is the wall thermal resistance. The Wilson's method [12] was applied to calculate $h_{w,h}$ and $h_{w,c}$.

3.2. Two phase condensation heat transfer

The procedures to calculate the condensation heat transfer coefficient of the refrigerant flow are described in the following. Firstly, the total heat transfer rate between the counter flows in the PHE is calculated from the cold water side

$$Q_w = W_{w,c} c_{p,w} (T_{w,c,o} - T_{w,c,i}) \tag{11}$$

Then, the refrigerant vapor quality entering the test section is evaluated from the energy balance for the pre-evaporator. Based on the temperature drop on the water side the heat transfer in the pre-evaporator is calculated from the relation

$$Q_{w,p} = W_{w,p} c_{p,w} (T_{w,p,i} - T_{w,c,i}) \tag{12}$$

While the heat transfer to the refrigerant in the pre-evaporator is the summation of the sensible heat transfer (for the temperature rise of the refrigerant to the saturated value) and latent heat transfer (for the evaporation of the refrigerant).

$$Q_{w,p} = Q_{sens} + Q_{lat} \tag{13}$$

where

$$Q_{sens} = W_r c_{p,r} (T_{r,sat} - T_{r,p,i}) \tag{14}$$

$$Q_{lat} = W_r i_{fg} X_{p,o} \tag{15}$$

The above equations can be combined to evaluate the refrigerant quality at the exit of the pre-evaporator, that is considered to be the same as the vapor quality of the refrigerant entering the test section. Specifically,

$$X_i = X_{p,o} = \frac{1}{i_{fg}}\left(\frac{Q_{w,p}}{W_r} - c_{p,r}(T_{r,sat} - T_{r,p,i})\right) \tag{16}$$

The change in the refrigerant vapor quality in the test section is then deduced from the energy transfer from the refrigerant to the water flow in the test section Q_w:

$$\Delta X = \frac{Q_w}{i_{fg} W_r} \tag{17}$$

The determination of the overall heat transfer coefficient for the condensation of R-134a in the PHE is similar to that for the single phase heat transfer, i.e.,

$$U = \frac{Q_w}{A\,\text{LMTD}} \tag{18}$$

The log mean temperature difference (LMTD) is again determined from the inlet and exit temperatures in the two channels:

$$\text{LMTD} = \frac{(\Delta T_1 - \Delta T_2)}{\ln(\Delta T_1/\Delta T_2)} \tag{19}$$

where

$$\Delta T_1 = T_{r,o} - T_{w,c,i} \tag{20}$$

$$\Delta T_2 = T_{r,i} - T_{w,c,o} \tag{21}$$

with $T_{r,i}$ and $T_{r,o}$ being the saturated temperatures of R-134a corresponding respectively to the inlet and outlet pressures in the refrigerant flow in the PHE. Finally, the condensation heat transfer coefficient in the flow of R-134a is evaluated from the equation

$$\frac{1}{h_r} = \frac{1}{U} - \frac{1}{h_{w,c}} - R_{wall}A \tag{22}$$

where $h_{w,c}$ is determined from the empirical correlation for the single phase water to water heat transfer.

3.3. Friction factor

To evaluate the friction factor associated with the R-134a condensation in the refrigerant channel, the frictional pressure drop ΔP_f was first calculated by subtracting the pressure losses at the test section inlet and exit manifolds and ports $(\Delta P)_{man}$, then adding the deceleration pressure rise during the R-134a condensation ΔP_{de} and the elevation pressure rise ΔP_{de} from the measured total pressure drop ΔP_{exp} for the refrigerant channel. Note that for the vertically downward refrigerant flow studied here the elevation pressure rise should be added in evaluating ΔP_f. Thus

$$\Delta P_f = \Delta P_{exp} - (\Delta P)_{man} + \Delta P_{de} + \Delta P_{ele} \tag{23}$$

The deceleration and elevation pressure rises were estimated by the homogeneous model for the two phase gas–liquid flow [14],

$$\Delta P_{de} = G^2 v_{fg} \Delta X \tag{24}$$

$$\Delta P_{ele} = \frac{gL}{v_m} \tag{25}$$

where w_m is the mean specific volume of the vapor–liquid mixture in the refrigerant channel when they are homogeneously mixed and is given as

$$v_m = [X_m v_g + (1 - X_m) v_l] = (v_l + X_m v_{fg}) \tag{26}$$

The pressure drop in the inlet and outlet manifolds and ports was empirically suggested by Shah and Focke [9]. It is approximately 1.5 times the head due to the flow expansion at the channel inlet

$$(\Delta P)_{man} \approx 1.5 \left(\frac{u_m^2}{2 v_m} \right)_i \tag{27}$$

where u_m is the mean flow velocity. With the homogeneous model the mean velocity is

$$u_m = G v_m \tag{28}$$

Based on the above estimation the deceleration pressure rise, the pressure losses at the test section inlet and exit manifolds and ports, and the elevation pressure rise were found to be rather small. The frictional pressure drop ranges from 93% to 99% of the total pressure drop measured. According to the definition

$$f_{tp} \equiv - \frac{\Delta P_f D_h}{2 G^2 v_m L} \tag{29}$$

the friction factor for the condensation of R-134a in the PHE is obtained.

3.4. Uncertainty analysis

To estimate the uncertainties of the experimental results, an uncertainty analysis was carried out. Kline and McClintock [15] proposed a formula for evaluating the uncertainty. The detailed results of the uncertainty analysis are summarized in Table 1.

4. Results and discussion

From the initial single phase water to water heat transfer test for the plate heat exchanger, the convection heat transfer coefficient in the cold side was correlated by the least square method as

$$Nu = 0.2121 Re^{0.78} Pr^{1/3} \tag{30}$$

In what follows the effects of the mass flux, average imposed heat flux and system pressure on the measured data are to be examined in detail. Before presenting the results the repeatability of the measured data was noted to be good.

Table 1
Parameters and estimated uncertainties

Parameter	Uncertainty
Length, width and thickness (m)	± 0.00005
Area of the plate (m^2)	$\pm 7 \times 10^{-5}$
Temperature, T (°C)	± 0.2
ΔT (°C)	± 0.3
Pressure, P (MPa)	± 0.002
Pressure drop, ΔP (Pa)	± 200
Water flow rate, M_w (%)	± 2
Mass flux of refrigerant, G (%)	± 2
Heat flux of test section, q_w'' (%)	± 6.5
Heat transfer rate of pre-evaporator, $Q_{w,p}$ (%)	± 6.5
Vapor quality, X	± 0.03
Single phase water test heat transfer coefficient, h_w (%)	± 10
R-134a condensation heat transfer coefficient, h_r (%)	± 15
Friction factor, f_{tp} (%)	± 20

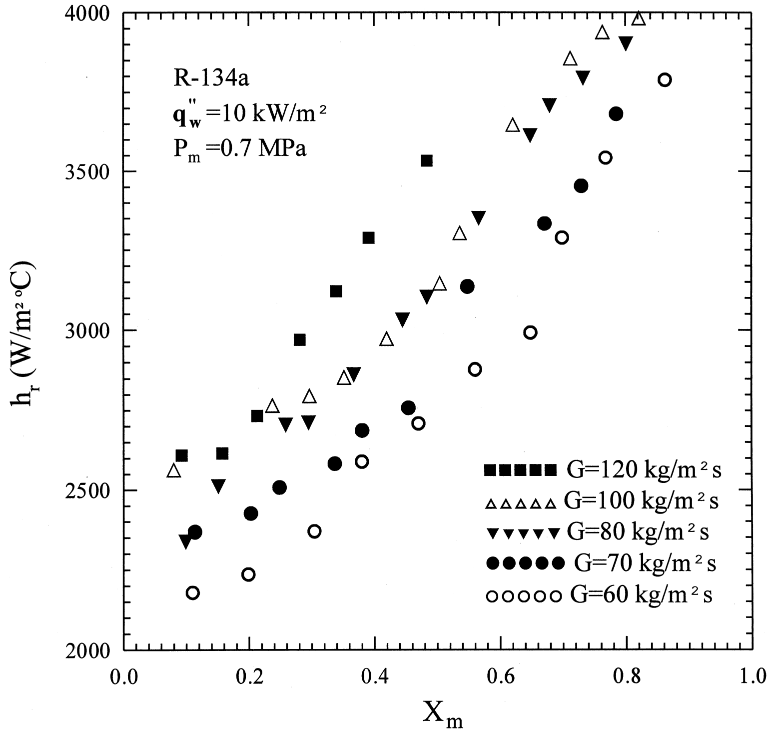

Fig. 3. Variations of condensation heat transfer coefficient with mean vapor quality for various mass fluxes at $P_m = 0.7$ MPa and $q_w'' = 10$ kW/m^2.

4.1. Two phase condensation heat transfer

Figure 3 shows the effects of the refrigerant mass flux on the measured R-134a condensation heat transfer coefficient at an average pressure of 0.7 MPa and an average imposed heat flux of 10 kW/m^2 for the mass flux ranging from 60 to 120 kg/m^2 s and the mean vapor quality varying from 0.08 to 0.86. The mean vapor quality X_m is the average vapor quality in the plate heat exchanger estimated from X_i and ΔX. These data indicate that at a given mass flux the condensation heat transfer coefficient almost increases linearly with the mean vapor quality of the refrigerant in the PHE. This increase is rather significant. For instance, at 60 kg/m^2 s the condensation heat transfer coefficient at the quality X_m of 0.8 is about 70% larger than that at 0.1. This obviously results from the simple fact that at a higher X_m the liquid film on the surface was thinner and the condensation rate is thus higher. But a rise in the mass flux does not always produce a comparable increase in the condensation heat transfer. Specifically, the h_r values for $G = 120$ kg/m^2 s are the highest except at low qualities, $X_m < 0.25$. At $G = 80$ and 100 kg/m^2 s the h_r values differ only slightly. They are larger than those for $G = 60$ and 70 kg/m^2 s to some degree. A close inspection of the data in Fig. 3 reveals that at a given G there exists a sharp rise in the condensation heat transfer coefficient at a certain X_m. For a higher mass flux the sharp change appears at a lower vapor quality. For example, at $G = 60$ kg/m^2 s the change occurs at $X_m \approx 0.65$ and at $G = 80$ kg/m^2 s the change is at $X_m \approx 0.55$–0.6. This sharp change in h_r is attributed to the flow pattern change. Specifically, when the vapor quality decreases the vapor flow may become laminar instead of being turbulent due to the smaller vapor flow rate.

Next, results are presented to illustrate the effects of the average imposed heat flux on the condensation heat transfer coefficient. Figure 4 shows the R-134a condensation heat transfer coefficients at three different heat fluxes (= 10, 13 and 16 kW/m^2) at 0.7 MPa and 60 kg/m^2 s. Note that the quality-averaged condensation heat transfer coefficients at 13 and 16 kW/m^2 are respectively about 6% and 10% larger than that at 10 kW/m^2. Compared with the mass flux effects shown in Fig. 3, the heat flux has a smaller effect on the condensation heat transfer coefficient in the high vapor quality region. Again at a certain X_m a sharp rise in h_r with the mean vapor quality was observed for each heat flux. Note that these large changes in h_r appear for X_m around 0.6 for all three cases.

Then, the effects of the average refrigerant pressure on the R-134a condensation heat transfer are examined. Figure 5 presents the data for the condensation heat

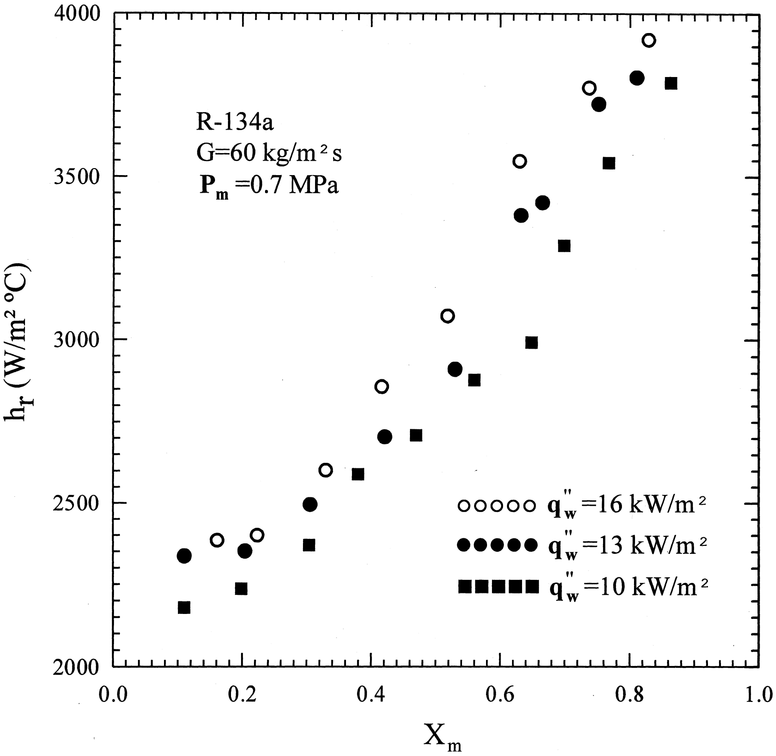

Fig. 4. Variations of condensation heat transfer coefficient with mean vapor quality for various heat fluxes at $G = 60$ kg/m^2 s and $P_m = 0.7$ MPa.

transfer coefficient at the heat flux of 10 kW/m^2 and mass flux of 60 kg/m^2 s for three system pressures of 0.7, 0.8 and 0.9 MPa which respectively correspond to the saturated temperatures of 26.7°C, 31.3°C and 35.5°C for R-134a. The results indicate that an increase in the system pressure leads to a slight reduction in the condensation heat transfer. Specifically, the mean heat transfer coefficient at 0.9 MPa is about 5 to 10% smaller than that at 0.7 MPa. This is conjectured to be mainly resulting from a 5.4% reduction in the conductivity of liquid film for the R-134a pressure raised from 0.7 to 0.9 MPa.

Finally, it is necessary to compare the present data for the R-134a condensation heat transfer coefficient in the plate heat exchanger to those in circular pipes reported in the literature. Due to the limited availability of the data for pipes with the same ranges of the parameters covered in the present study. The comparison is only possible for a few cases. This is illustrated in Fig. 6, in which our data are compared with those from Eckels and Pate [3]. Note that the data from Eckels and Pate are average h_r values measured in a long pipe of 3.67 m in length with the vapor quality varying from 0.9 at the pipe inlet to 0.1 at the exit. The comparison in Fig. 6 manifests that even at a lower mass flux of 100 kg/m^2 s the R-134a condensation heat transfer coefficient for the plate heat exchanger is about 25% in average higher than that for the circular pipe with the mass flux of 130 kg/m^2 s.

4.2. Two phase frictional pressure drop

The changes of the frictional pressure drop with the vapor quality and mass flux, as shown in Fig. 7, are similar to those for the condensation heat transfer coefficient in Fig. 3. Note that the variation of ΔP_f with the vapor quality is much larger than the heat transfer coefficient. At $G = 80$ kg/m^2 s the frictional pressure drop can be approximately increased by six times for X_m raised from 0.2 to 0.8. Figure 8 shows the effects of the wall heat flux on the frictional pressure drop. These data indicate that some increase in the pressure drop results when the heat flux is raised from 10 to 13 kW/m^2. But a further rise to 16 kW/m^2 does not result in a noticeable difference in ΔP_f. Figure 9 manifests the effects of the system pressure on the frictional pressure drop. Note that the system pressure has a very small effect on the frictional pressure drop in the PHE.

4.3. Correlation equations

To facilitate the use of the plate heat exchanger as a condenser, correlating equations for the dimensionless

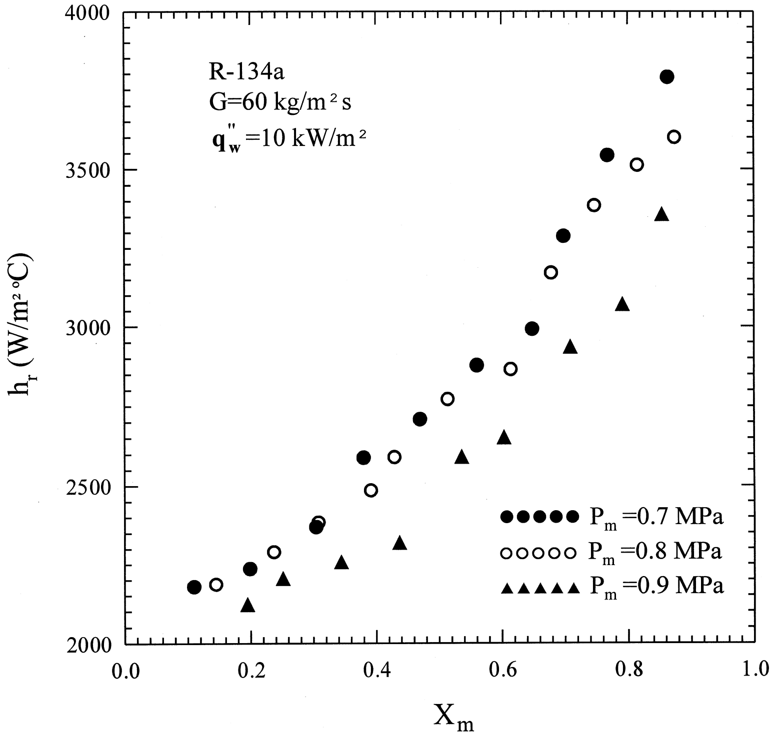

Fig. 5. Variations of condensation heat transfer coefficient with mean vapor quality for various pressures at $G = 60$ kg/m^2 s and $q_w'' = 10$ kW/m^2.

condensation heat transfer coefficient and friction factor based on the present data are provided. They are

$$Nu = \frac{h_r D_h}{k_l} = 4.118 Re_{eq}^{0.4} Pr_l^{1/3} \tag{31}$$

and

$$f_{tp} Re^{0.4} Bo^{-0.5} \left(\frac{p_m}{P_c}\right)^{-0.8} = 94.75 Re_{eq}^{-0.0467} \tag{32}$$

where P_c is the critical pressure of R-134a (4.064 MPa), Re_{eq} is the equivalent Reynolds number and Bo is the boiling number. Re_{eq} and Bo are defined as

$$Re_{eq} = \frac{G_{eq} D_h}{\mu_l} \tag{33}$$

$$Bo = \frac{q_w''}{G i_{fg}} \tag{34}$$

in which

$$G_{eq} = G\left[1 - X_m + X_m \left(\frac{\rho_l}{\rho_v}\right)^{1/2}\right] \tag{35}$$

Here G_{eq} was proposed by Akers et al. [7] and is an equivalent mass flux which is a function of the R-134a mass flux, mean quality and densities at the saturated condition. Figure 10 shows the comparison of the proposed condensation heat transfer correlation to the present data, indicating that most of the experimental values are within $\pm 15\%$. Figure 11 illustrates the comparison of the proposed correlation for the friction factor to the present data. It is found that the average deviation is about 13.3% between the f_{tp} correlation and the data.

5. Concluding remarks

An experimental investigation has been conducted in the present study to measure the condensation heat transfer coefficient and pressure drop of R-134a in a plate heat exchanger. The effects of the mass flux of R-134a, average imposed heat flux, system pressure and vapor quality of R-134a on the measured data were examined in detail. The results show that the condensation heat transfer coefficient and pressure drop normally increase with the refrigerant mass flux. But the increase in the pressure drop is more significant. Note that a sharp rise in the heat transfer coefficient was found with a small increase in the vapor quality during condensation for a lower mass flux but not clearly for a higher mass flux. A rise in the average imposed heat flux results in slightly better condensation heat transfer accompanying with a larger pressure drop. Finally, it was noted that at a higher system pressure the condensation heat transfer coefficient

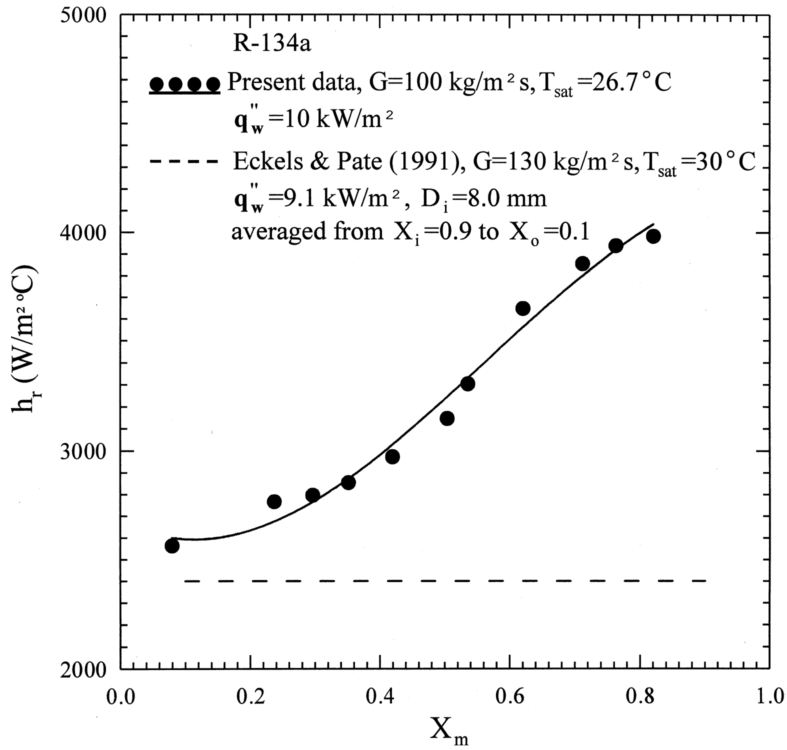

Fig. 6. Comparison of the present heat transfer data for the plate heat exchanger with those for circular pipe from [3].

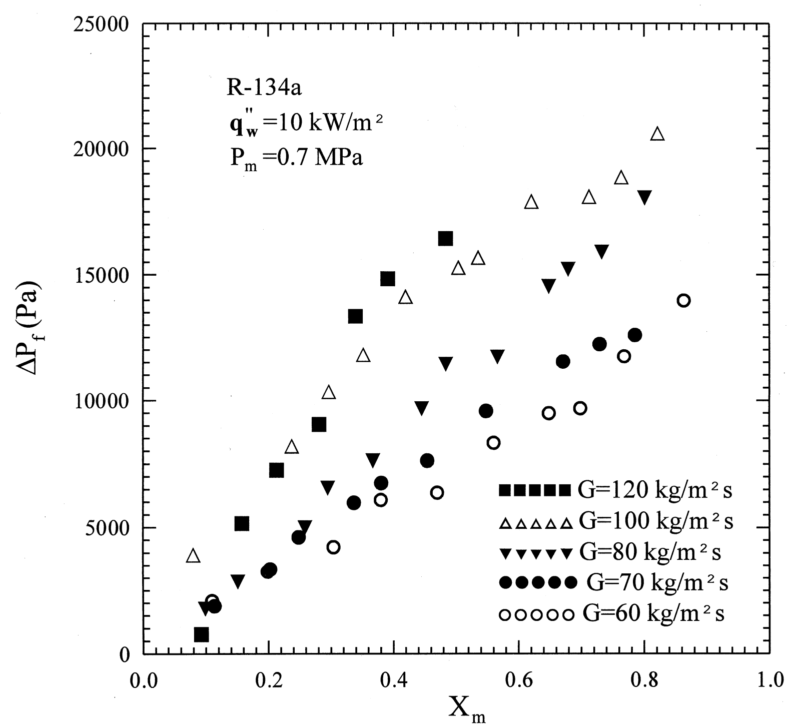

Fig. 7. Variations of frictional pressure drop with mean vapor quality for various mass fluxes at $P_m = 0.7$ MPa and $q_w = 10$ kW/m^2.

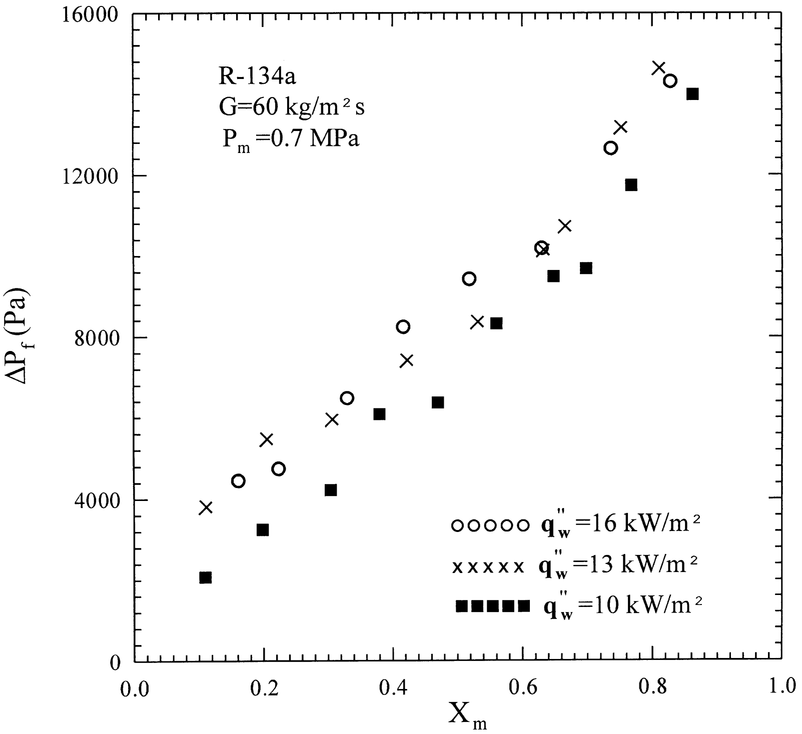

Fig. 8. Variations of frictional pressure drop with mean vapor quality for various heat fluxes at $G = 60$ kg/m^2 s and $P_m = 0.7$ MPa.

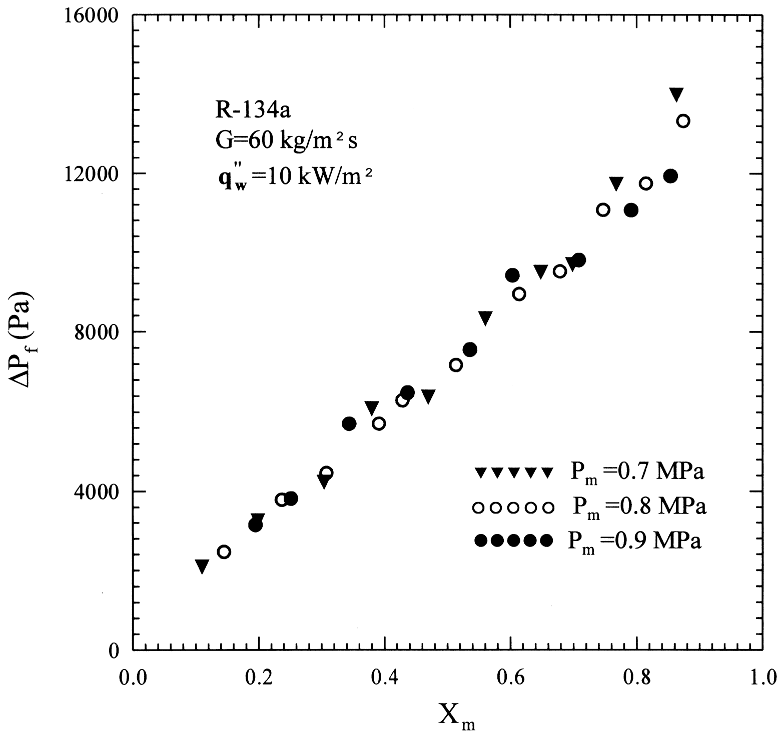

Fig. 9. Variations of frictional pressure drop with mean vapor quality for various pressures at $G = 60$ kg/m^2 s and $q_w'' = 10$ kW/m^2.

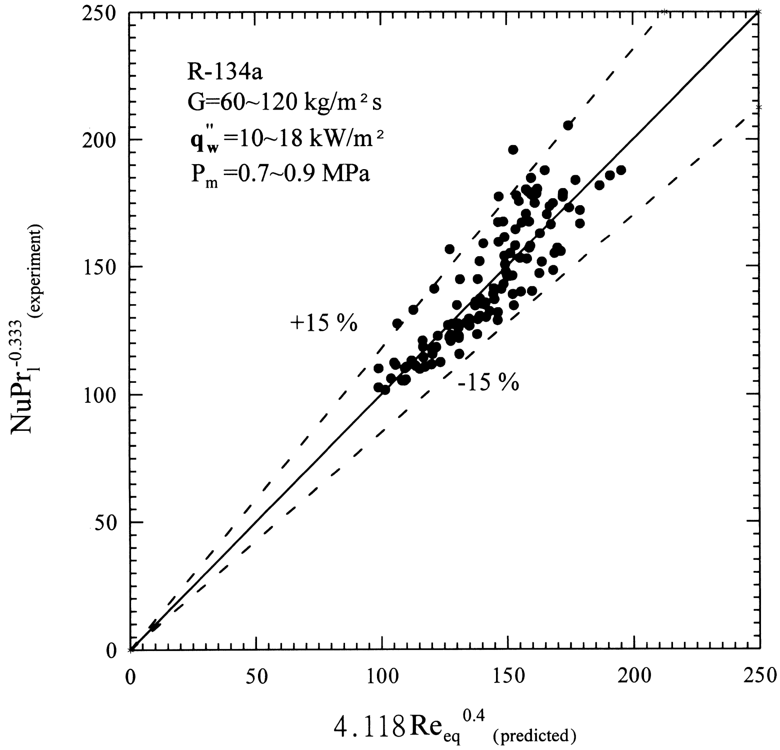

Fig. 10. Comparison of the proposed correlation for Nusselt number with the present data.

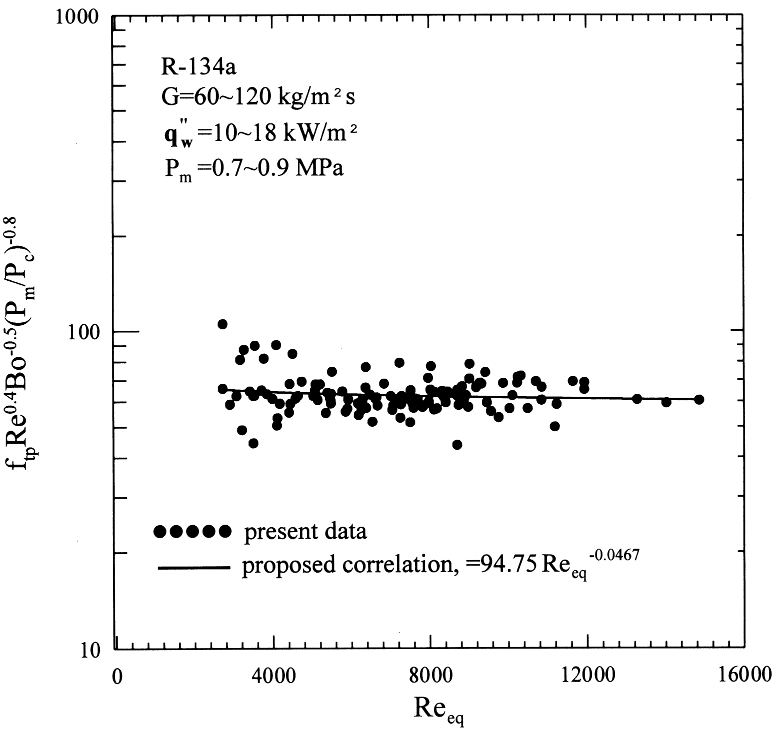

Fig. 11. Comparison of the proposed correlation for friction factor with the present data.

is slightly lower. But the effects of changing the system pressure on the pressure drop are small. Correlations were also proposed for the measured heat transfer coefficients and pressure drops in terms of the Nusselt number and friction factor.

Acknowledgements

The financial support of this study by the engineering division of National Science Council of Taiwan, through contract NSC85-2221-E-009-046 and Dr. B.C. Yang's help during construction of the present experimental facility are greatly appreciated.

References

[1] L.M. Schlager, M.B. Pate, A.E. Bergles, Evaporation and condensation heat transfer and pressure drop in horizontal, 12.7 mm microfin tubes with refrigerant 22, J. Heat Transfer 112 (1990) 1041–1047.

[2] L.M. Schlager, M.B. Pate, A.E. Bergles, Heat transfer and pressure drop during evaporation and condensation of R22 in horizontal micro-fin tubes, Int. J. Refrig. 12 (1989) 6–14.

[3] S.J. Eckels, M.B. Pate, An experimental comparison of evaporation and condensation heat transfer coefficients for HFC-134a and CFC-12, Int. J. Refrig. 14 (1991) 70–77.

[4] K. Torikoshi, T. Ebisu, Evaporation and condensation heat transfer characteristics of R-134a, R-32 and a mixture of R-32/R-134a inside a tube, ASHRAE Trans. 99 (1) (1993) 90–96.

[5] X. Liu, Condensing and evaporating heat transfer and pressure drop characteristics of HFC-134a and HCFC-22, J. Heat Transfer 119 (1997) 158–163.

[6] L.M. Chamra, R.L. Webb, Advanced micro-fin tubes for condensation, Int. J. Heat Mass Transfer 39 (1996) 1839–1846.

[7] W.W. Akers, H.A. Dean, O. Crosser, Condensation heat transfer within horizontal tubes, Chem. Eng. Prog. 54 (10) (1958) 89–90.

[8] M.M. Shah, A general correlation for heat transfer during film condensation inside pipes, Int. J. Heat Mass Transfer 22 (1979) 547–556.

[9] R.K. Shah, W.W. Focke, Plate heat exchangers and their design theory, in: R.K. Shah, E.C. Subbarao, R.A. Mashelkar (Eds.), Heat Transfer Equipment Design, Hemisphere, Washington, DC, 1988, pp. 227–254.

[10] S.G. Kandlikar, R.K. Shah, Multipass plate heat exchangers-effectiveness-NTU results and guidelines for selecting pass arrangements, J. Heat Transfer 111 (1989) 300–313.

[11] S.G. Kandlikar, R.K. Shah, Asymptotic effectiveness-NTU formulas for multipass plate heat exchangers, J. Heat Transfer 111 (1989) 314–321.

[12] E.E. Wilson, A basis for traditional design of heat transfer apparatus, Trans. ASME 37 (1915) 47–70.

[13] R.K. Shah, A.S. Wanniarachchi, Plate heat exchanger design theory in industry heat exchanger, in: J.-M. Buchlin (Ed.), Lecture Series, No. 1991-04, Von Karman Institute for Fluid Dynamics, Belgium, 1992.

[14] J.G. Collier, Convective Boiling and Condensation, 2nd ed., McGraw-Hill, 1982.

[15] S.J. Kline, F.A. McClintock, Describing uncertainties in single-sample experiments, Mech. Eng. 75 (1) (1953) 3–12.